CSIAM Trans. Appl. Math.
doi: 10.4208/csiam-am.SO-2023-0039

Vol. **x**, No. x, pp. 1-25
xx 2025

An Accelerated Spectral Perry-Type Conjugate Gradient Projection Method for Unconstrained Nonlinear Equations with Applications

Pengjie Liu[1], Xiaoyu Wu[1], Hu Shao[1,2,*] and Ting Wu[3,*]

[1] *School of Mathematics, China University of Mining and Technology, Xuzhou 221116, P.R. China.*
[2] *Jiangsu Center for Applied Mathematics (CUMT), China University of Mining and Technology, Xuzhou 221116, P.R. China.*
[3] *School of Mathematics, Nanjing University, Nanjing 210093, P.R. China.*

Received 3 August 2023; Accepted 28 July 2025

Abstract. In this paper, we propose an accelerated spectral Perry-type conjugate gradient projection method for solving systems of unconstrained nonlinear equations. The spectral parameter is generated using an accelerated gradient-descent method, which ensures that the proposed search direction always satisfies the sufficient descent condition. By incorporating a self-adaptive strategy into the optimal Perry conjugate parameter, the proposed search direction possesses the trust region property independent of any line search. Additionally, the proposed method incorporates an inertial extrapolation step to enhance computational performance. The global convergence of the proposed method is theoretically established without requiring monotonicity or pseudo-monotonicity of the underlying mapping. Numerical experiments on systems of unconstrained nonlinear equations and image de-blurring problems demonstrate the effectiveness of the proposed method.

AMS subject classifications: 65K05, 90C30

Key words: Unconstrained nonlinear equations, derivative-free projection method, convergence analysis.

1 Introduction

The system of nonlinear equations (SoNE) arises in many practical and scientific applications, including compressive sensing [54, 55, 57] and traffic assignment [29, 33]. Due to its significance, the research on iterative methods for solving SoNEs has garnered exten-

*Corresponding author. *Email addresses:* liupengjie2019@163.com (P. Liu), shaohu@cumt.edu.cn (H. Shao), xiaoyuwu0218@163.com (X. Wu), tingwu@nju.edu.cn (T. Wu)

sive attention. In recent decades, numerous iterative methods for solving SoNEs have been developed, predominantly falling into two categories: derivative-based projection methods and derivative-free projection (DFP) methods. The former category comprises Newton-type method [44, 64], quasi-Newton method [4, 66], Gauss-Newton method [11, 25], semi-smooth Newton method [53], Levenberg-Marquardt method [58], and others. These methods usually exhibit rapid convergence, provided that the initial point is in close proximity to the solution set. However, they require the computation and/or storage of the Jacobian or its approximation at each iteration, making them less suitable for solving large-scale SoNEs. In contrast, the derivative-free category is particularly suitable for addressing large-scale SoNEs due to its derivative-free nature. Hence, in this paper, we focus on the conjugate gradient (CG) projection method within the latter category.

Given the excellent performance of the conjugate gradient method in solving unconstrained optimization problems, several researchers have combined it with the hyperplane projection method [44] to solve SoNEs. Cheng [5] expanded upon the classical Polak-Ribière-Polyak CG method [40, 41] to develop a derivative-free CG projection method for solving monotone SoNEs. Sun and Liu [47] generalized the hybrid CG method proposed by Jian *et al.* [22], applied it to constrained monotone SoNEs, and established the convergence of the algorithm without assuming Lipschitz continuity for the underlying mapping. To expand the applicability and improve the effectiveness of the Dai-Yuan CG method [8], Liu and Feng [26] proposed a spectral Dai-Yuan-type CG projection method, in which the spectral parameter is carefully chosen to ensure that the search direction satisfies the descent condition. Awwal *et al.* [2] introduced an extension of the spectral Hestenes-Stiefel CG-type method for solving monotone SoNEs with convex constraints. They also applied this method to signal recovery problems. By combining the Dai-Liao-based CG projection method [1] with an adapted version of the quasi-Newton modified Stanimirović-Miladinović (MSM) scheme [21], Ivanov *et al.* [20] proposed a modified CG projection method with an acceleration parameter to solve unconstrained monotone SoNEs. Clearly, most of these proposed methods are variants of well-known CG methods. More related methods can be found in [9,15,27,28,35,51,56,57,67,68] and the references therein.

With the rapid growth in the scale of SoNEs, it has become essential to design iterative schemes with fast convergence. The inertial step was originally proposed in the heavy ball method [39], which is based on the implicit discretization of a second-order differential equation. Indeed, the accelerated gradient method is analogous to the concept of momentum in physics. It builds upon gradient descent and has emerged as a widely recognized and effective strategy for accelerating convergence. However, unlike the heavy ball method, the accelerated gradient method first applies a momentum impulse to the current point x_k to generate an auxiliary point y_k, and then performs a gradient descent step at y_k. A key feature of the inertial step is that it leverages information from the two previous iterations to generate the next iterate. As noted by Zhu *et al.* [69], the momentum mechanism effectively reduces oscillations and facilitates faster convergence of iterates toward the optimal solution. Given the promising performance of methods in-

corporating inertial terms in other optimization problems, several researchers have extended DFP methods by integrating inertial steps for solving SoNEs. For example, by integrating an inertial step into the DFP method, Ibrahim *et al.* [19] proposed an inertial three-term DFP method for solving constrained monotone SoNEs, and applied it to signal recovery problems. Later, Ibrahim *et al.* [16] incorporated an inertial extrapolation step into the three-term search direction [48], thereby introducing a new inertial three-term DFP method for solving constrained monotone SoNEs. Building upon the inertial acceleration technique, Jian *et al.* [23] proposed a family of inertial DFP methods to solve constrained pseudo-monotone SoNEs, where the search direction was only required to satisfy the sufficient descent condition. Recently, Wu *et al.* [52] extended the well-known Dai-Kou CG method [7] for constrained monotone SoNEs by introducing an effective spectral parameter via a quasi-Newton strategy. They also established the convergence and convergence rate results of the method with inertial acceleration, under a suitable restart condition. For more inertial methods for solving unconstrained or constrained SoNEs, see [18, 24, 29, 31, 32, 34, 62].

Motivated by the above discussion, we extend the optimal Perry conjugate parameter [42] by incorporating an adaptation of the quasi-Newton MSM scheme [21] and an inertial acceleration strategy. As a result, we propose an accelerated spectral Perry-type CG projection (ASPCGP) method for solving unconstrained SoNEs. In essence, the ASPCGP method can be viewed as a natural extension of the Perry-type CG method. Moreover, the incorporation of the following features further enhances the practical appeal of the ASPCGP method.

- To overcome the theoretical limitations of the optimal Perry conjugate parameter [42] and improve the algorithm's numerical performance, we begin by modifying it through the implementation of a self-adaptive strategy. Subsequently, the spectral parameter in the search direction is derived using the accelerated gradient-descent method, specifically the MSM scheme.
- Regarding the obtained search direction, not only is the sufficient descent condition always satisfied, but the trust region property is also guaranteed through the use of a valid judgment condition and the reinitialization of the parameter, without the need for any line search. Moreover, it is demonstrated that the global convergence of the ASPCGP method is guaranteed, even in the absence of monotonicity or pseudo-monotonicity in the underlying mapping.
- Numerical experiments are conducted to solve large-scale unconstrained SoNEs and restore blurred images. The results demonstrate the excellent performance and potential applicability of the ASPCGP method.

The remainder of this paper is organized as follows. Section 2 presents the proposed method. Section 3 provides the global convergence analysis. In Section 4, we report numerical results on unconstrained SoNEs and practical applications in image restoration. Finally, conclusions are drawn in Section 5.

2 Motivation and algorithm

In this section, we introduce a spectral Perry-type CG projection method for solving unconstrained SoNEs. The problem to be solved is formulated as

$$E(x)=0, \tag{2.1}$$

where the mapping $E:\mathbb{R}^n\to\mathbb{R}^n$ is L-Lipschitz continuous. The mapping E is said to be L-Lipschitz continuous if there exists a constant $L>0$ such that $\|E(x)-E(y)\|\leq L\|x-y\|$ for any x, $y\in\mathbb{R}^n$. Here, $\|\cdot\|$ denotes the Euclidean norm in $\mathbb{R}^n$.

We begin by briefly reviewing Perry CG method. In 1978, Perry [38] proposed a modified CG method based on the ideas of the quasi-Newton method and the Fletcher-Reeves CG method [13], for solving an unconstrained optimization problem of the form $\min\{f(x)\,|\,x\in\mathbb{R}^n\}$. The corresponding search direction and conjugate parameter are defined as

$$d_k=\begin{cases}-\nabla f(x_k), & \text{if} \quad k=0,\\ -\nabla f(x_k)+\beta_k^{\mathrm{P}}s_{k-1}, & \text{if} \quad k\geq 1,\end{cases} \tag{2.2}$$

$$\beta_k^{\mathrm{P}}=\frac{\nabla f(x_k)^{\top}(\hat{p}_{k-1}-s_{k-1})}{s_{k-1}^{\top}\hat{p}_{k-1}}, \tag{2.3}$$

where $s_{k-1}=x_k-x_{k-1}$ and $\hat{p}_{k-1}=\nabla f(x_k)-\nabla f(x_{k-1})$. The Perry CG method has attracted considerable attention in the literature due to its efficiency and robust numerical performance. Furthermore, various researchers have enhanced and extended it to solve both unconstrained and constrained SoNEs. For example, Waziri *et al.* [50] extended a modified version of the Perry CG method to solve unconstrained SoNEs. Subsequently, Awwal *et al.* [3] proposed a Perry-type DFP method for solving constrained SoNEs, which was based on the Broyden-Fletcher-Goldfarb-Shanno (BFGS) quasi-Newton method and incorporated a modified Perry-type parameter. Preliminary numerical results have demonstrated the superiority of this method. Recently, Sabi'u *et al.* [42] derived an optimal parameter for the scaled Perry-type CG projection method by minimizing the gap between the maximum and minimum eigenvalues of the search direction matrix. Notably, their proposed method does not rely on any predefined fixed parameters.

In 2021, the MSM system [21] was utilized as an acceleration technique in the solution of the unconstrained monotone SoNE by Ivanov *et al.* [20], resulting in the development of an efficient algorithm. The adaptation of the MSM method to address the problem (2.1) can be expressed as

$$x_{k+1}=x_k-\left(\tau_k+\tau_k^2-\tau_k^3\right)\left(\Gamma_k^{\mathrm{MSM}}\right)^{-1}E(x_k), \tag{2.4}$$

where the scalar $\Gamma_k^{\mathrm{MSM}}\in\mathbb{R}$ denotes the acceleration parameter and is strictly positive. The value $\tau_k\in(0,1]$ is selected according to the step-length obtained from the line search.

Define $\zeta_k = 1+\tau_k-\tau_k^2$, which implies that $\zeta_k \in [1,5/4]$. This parameter is introduced to provide additional acceleration. Then, the search direction in (2.4) is defined as

$$d_k^{\mathrm{MSM}} = -\zeta_k \left(\Gamma_k^{\mathrm{MSM}}\right)^{-1} E(x_k). \tag{2.5}$$

Here, under the assumption that $E(x)$ is differentiable, we employ the first-order Taylor expansion to approximate $E(x_{k+1})$ and derive $\Gamma_{k+1}^{\mathrm{MSM}}$, i.e.,

$$\begin{aligned} E(x_{k+1}) &\approx E(x_k) + \nabla E(\xi)(x_{k+1}-x_k) \\ &\approx E(x_k) + \nabla E(\xi)\tau_k d_k^{\mathrm{MSM}} \\ &\approx E(x_k) - \nabla E(\xi)\tau_k\zeta_k \left(\Gamma_k^{\mathrm{MSM}}\right)^{-1} E(x_k), \quad \xi \in [x_k, x_{k+1}]. \end{aligned} \tag{2.6}$$

As proposed by Ivanov *et al.* [21], $\nabla E(\xi)$ is approximated by $\Gamma_{k+1}^{\mathrm{MSM}} I$. Based on (2.6), this leads to

$$E(x_{k+1}) - E(x_k) \approx -\Gamma_{k+1}^{\mathrm{MSM}} \tau_k \zeta_k \left(\Gamma_k^{\mathrm{MSM}}\right)^{-1} E(x_k). \tag{2.7}$$

Given the aforementioned relation and $p_k = E(x_{k+1}) - E(x_k)$, we conclude that

$$p_k = -\Gamma_{k+1}^{\mathrm{MSM}} \tau_k \zeta_k \left(\Gamma_k^{\mathrm{MSM}}\right)^{-1} E(x_k). \tag{2.8}$$

After multiplying both sides of (2.8) by $p_k^\top$ and simplifying, we have

$$\Gamma_{k+1}^{\mathrm{MSM}} = -\frac{\Gamma_k^{\mathrm{MSM}} \|p_k\|^2}{\tau_k \zeta_k p_k^\top E(x_k)}. \tag{2.9}$$

To satisfy the second-order necessary/sufficient condition, any inappropriate values of $\Gamma_{k+1}^{\mathrm{MSM}} \le 0$ will be substituted with $\Gamma_{k+1}^{\mathrm{MSM}} = 1$ (as mentioned in [20, 21, 31, 46]). However, as described in [24], this may not fully ensure that the search direction satisfies the sufficient descent condition and the trust region property, both of which are crucial for theoretical analysis. Similar to the approach in [24], in this work, we further refine the parameter $\Gamma_{k+1}^{\mathrm{MSM}}$ to ensure its boundedness. Specifically, we set $\Gamma_{k+1}^{\mathrm{MSM}} = 1$ if $\Gamma_{k+1}^{\mathrm{MSM}} \le \Gamma_{\min}^{\mathrm{MSM}}$, and $\Gamma_{k+1}^{\mathrm{MSM}} = \Gamma_{\max}^{\mathrm{MSM}}$ if $\Gamma_{k+1}^{\mathrm{MSM}} \ge \Gamma_{\max}^{\mathrm{MSM}}$, where $\Gamma_{\min}^{\mathrm{MSM}}$ and $\Gamma_{\max}^{\mathrm{MSM}}$ are constants satisfying $0 < \Gamma_{\min}^{\mathrm{MSM}} \le 1 \le \Gamma_{\max}^{\mathrm{MSM}}$.

Herein, following Perry's perspective [38], we adopt the search direction derived from (2.2) and (2.3), along with the insights from Sabi'u *et al.* [42], to obtain the optimal Perry conjugate parameter, defined as

$$\beta_k^{\mathrm{OP}} = \frac{\nabla f(x_k)^\top (\hat{\eta}_{k-1} - \bar{\Lambda}_k^* s_{k-1})}{s_{k-1}^\top \hat{\eta}_{k-1}},$$

where

$$\bar{\Lambda}_k^* = \frac{s_{k-1}^\top \hat{\eta}_{k-1}}{\|s_{k-1}\|^2}, \quad \hat{\eta}_{k-1} = \hat{p}_{k-1} + r s_{k-1}$$

with $r > 0$. Considering the spectral CG projection method, we extend the optimal Perry-

type conjugate parameter β_k^{OP} for solving the unconstrained SoNE (2.1). The corresponding search direction is given by

$$d_k=\begin{cases}-E(x_k), & \text{if} \quad k=0,\\ -\theta_k^{\mathrm{EOP}}E(x_k)+\beta_k^{\mathrm{EOP}}s_{k-1}, & \text{if} \quad k\geq 1,\end{cases} \tag{2.10}$$

where the improved Perry-type conjugate parameter β_k^{EOP} with the following form:

$$\beta_k^{\mathrm{EOP}}=\begin{cases}\dfrac{E(x_k)^\top(\eta_{k-1}-\Lambda_k^* s_{k-1})}{s_{k-1}^\top\eta_{k-1}}, & \text{if} \quad s_{k-1}^\top p_{k-1}\geq 0,\\ \varrho\cdot\dfrac{\|E(x_k)\|}{\|s_{k-1}\|}, & \text{otherwise,}\end{cases} \tag{2.11}$$

where

$$\Lambda_k^*=\frac{s_{k-1}^\top\eta_{k-1}}{\|s_{k-1}\|^2}, \quad \eta_{k-1}=p_{k-1}+rs_{k-1}$$

with $r>0$, and $\varrho\geq 0$. Unlike the observation in [42], when the mapping E does not exhibit the desired monotonicity property, we employ the criterion $s_{k-1}^\top p_{k-1}\geq 0$ to ensure Λ_k^* is non-negative. Notably, to avoid the under-performing effect of using the negative gradient as the resulting self-adaptive direction, we do not abruptly set β_k^{EOP} to 0 when $s_{k-1}^\top p_{k-1}<0$. In the search direction given by (2.10), θ_k^{EOP} is a spectral coefficient that needs to be determined. Next, there is a straightforward way to obtain it. Specifically, denoting the one-dimensional manifold by

$$\mathcal{S}_k=\left\{-\theta_k^{\mathrm{EOP}}E(x_k)+\beta_k^{\mathrm{EOP}}s_{k-1}:\theta_k^{\mathrm{EOP}}\in\mathbb{R}\right\},$$

we select the vector in $\mathcal{S}_k$ that is closest to d_k^{MSM} in (2.5) as the current search direction. Then, we obtain the coefficient θ_k^{EOP} by solving the following minimization problem:

$$\theta_k^{\mathrm{EOP}}=\arg\min\left\{\left\|d_k^{\mathrm{MSM}}-d_k\right\|^2:d_k\in\mathcal{S}_k\right\},$$

i.e.

$$\theta_k^{\mathrm{EOP}}=\arg\min\left\{\left\|\zeta_k\left(\Gamma_k^{\mathrm{MSM}}\right)^{-1}E(x_k)-\theta_k^{\mathrm{EOP}}E(x_k)+\beta_k^{\mathrm{EOP}}s_{k-1}\right\|^2:\theta_k^{\mathrm{EOP}}\in\mathbb{R}\right\}.$$

Furthermore, we deduce that

$$\theta_k^{\mathrm{EOP}}=\zeta_k\left(\Gamma_k^{\mathrm{MSM}}\right)^{-1}+\beta_k^{\mathrm{EOP}}\frac{E(x_k)^\top s_{k-1}}{\|E(x_k)\|^2}. \tag{2.12}$$

Subsequently, based on the search direction defined by (2.9)-(2.12), and combining the inertial extrapolation step-length with the hyperplane projection technique, we describe the ASPCGP method for solving the unconstrained SoNE (2.1). Below, we provide the detailed steps involved in the ASPCGP method (Algorithm 1).

Algorithm 1. ASPCGP Method.

Step 0. Given two initial points, $x_0 = y_0 \in \mathbb{R}^n$, we define the following parameters: $\varepsilon > 0, r > 0, \varrho \geq 0, \Gamma_0^{\mathrm{MSM}} = 1, \varsigma \in (0,1], \rho \in (0,1), \sigma > 0, \mu > 0, \nu > 0, \gamma \in (0,2), \phi \in [0,1)$, and $0 < \Gamma_{\min}^{\mathrm{MSM}} \leq 1 \leq \Gamma_{\max}^{\mathrm{MSM}}$. Additionally, let $\{\epsilon_k\}$ be a control parameter sequence such that $\epsilon_k \in [0,1)$ and $\sum_{k=1}^{+\infty} \epsilon_k < +\infty$.

Step 1. If $\|E(x_0)\| (= \|E(y_0)\|) \leq \varepsilon$, then stop. Otherwise, set $k := 0$, and go to next step.

Step 2. Calculate the search direction d_k of the following form:

$$d_k = \begin{cases} -E(y_k), & \text{if} \quad k = 0, \\ -\theta_k^{\mathrm{EOP}} E(y_k) + \beta_k^{\mathrm{EOP}} s_{k-1}, & \text{if} \quad k \geq 1, \end{cases} \tag{2.13}$$

where

$$\beta_k^{\mathrm{EOP}} = \begin{cases} \dfrac{E(y_k)^\top (\eta_{k-1} - \Lambda_k^* s_{k-1})}{s_{k-1}^\top \eta_{k-1}}, & \text{if} \quad s_{k-1}^\top p_{k-1} \geq 0, \\ \varrho \cdot \dfrac{\|E(y_k)\|}{\|s_{k-1}\|}, & \text{otherwise,} \end{cases} \qquad \Lambda_k^* = \frac{s_{k-1}^\top \eta_{k-1}}{\|s_{k-1}\|^2}, \tag{2.14}$$

$$\theta_k^{\mathrm{EOP}} = \zeta_k \left(\Gamma_k^{\mathrm{MSM}}\right)^{-1} + \beta_k^{\mathrm{EOP}} \frac{E(y_k)^\top s_{k-1}}{\|E(y_k)\|^2}. \tag{2.15}$$

Stop if $d_k = 0$.

Step 3. Take $z_k = y_k + t_k d_k$, where $t_k = \varsigma \rho^{i_k}$ with i_k being the smallest nonnegative integer such that

$$-E(y_k + t_k d_k)^\top d_k \geq \sigma t_k \|d_k\|^2 \min\{\mu, \nu \|E(y_k + t_k d_k)\|\}, \tag{2.16}$$

and let $\tau_k = t_k$. If $\|E(z_k)\| \leq \varepsilon$, then stop.

Step 4. Compute

$$x_{k+1} = y_k - \gamma \xi_k E(z_k), \tag{2.17}$$

where

$$\xi_k = \frac{E(z_k)^\top (y_k - z_k)}{\|E(z_k)\|^2}. \tag{2.18}$$

If $\|E(x_{k+1})\| \leq \varepsilon$, then stop.

Step 5. Compute the inertial step-length ϕ_{k+1},

$$\phi_{k+1} = \begin{cases} \min\left\{\phi, \dfrac{\epsilon_{k+1}}{\|x_{k+1} - x_k\|^2}\right\}, & \text{if} \quad x_{k+1} \neq x_k, \\ 0, & \text{otherwise.} \end{cases} \tag{2.19}$$

Step 6. Let the inertial extrapolation point as $y_{k+1}=x_{k+1}+\phi_{k+1}(x_{k+1}-x_k)$. If $\|E(y_{k+1})\|\leq\varepsilon$, then stop.

Step 7. Compute $s_k=y_{k+1}-y_k$ and $p_k=E(y_{k+1})-E(y_k)$ and put $\zeta_k=1+\tau_k-\tau_k^2$. Determine $\Gamma_{k+1}^{\mathrm{MSM}}$ using

$$\Gamma_{k+1}^{\mathrm{MSM}}=-\frac{\Gamma_k^{\mathrm{MSM}}\|p_k\|^2}{\tau_k\zeta_k p_k^\top E(y_k)}.$$

We set $\Gamma_{k+1}^{\mathrm{MSM}}=1$ if $\Gamma_{k+1}^{\mathrm{MSM}}\leq\Gamma_{\min}^{\mathrm{MSM}}$, and $\Gamma_{k+1}^{\mathrm{MSM}}=\Gamma_{\max}^{\mathrm{MSM}}$ if $\Gamma_{k+1}^{\mathrm{MSM}}\geq\Gamma_{\max}^{\mathrm{MSM}}$.

Step 8. Compute $\eta_k=p_k+rs_k$. Set $k:=k+1$, and return to Step 2.

Remark 2.1.

(i) In the improved parameter β_k^{EOP}, the choice of ϱ is an important consideration. It can either be a fixed value or dynamically updated based on the available iteration information.

(ii) Assuming that the search direction obtained from (2.13)-(2.15) satisfies the descent condition, the adaptive line search (2.16) is well-defined. A detailed proof of this result can be found in [30, Lemma 2].

(iii) From (2.19), we have $0\leq\phi_k\leq\phi<1$, and

$$\phi_k\|x_k-x_{k-1}\|^2\leq\epsilon_k,\quad\forall k\geq1, \tag{2.20}$$

which further implies

$$\sum_{k=1}^{+\infty}\phi_k\|x_k-x_{k-1}\|^2\leq\sum_{k=1}^{+\infty}\epsilon_k<+\infty. \tag{2.21}$$

The following lemma demonstrates that the search direction d_k, obtained from (2.13)-(2.15), satisfies the desirable sufficient descent condition, independent of any specific line search.

Lemma 2.1. *For all $k\geq0$, d_k satisfies the sufficient descent condition, i.e.,*

$$E(y_k)^\top d_k\leq-\left(\Gamma_{\max}^{\mathrm{MSM}}\right)^{-1}\|E(y_k)\|^2. \tag{2.22}$$

Proof. Since $d_0=-E(y_0)$, we have

$$E(y_0)^\top d_0=-\|E(y_0)\|^2\leq-\left(\Gamma_{\max}^{\mathrm{MSM}}\right)^{-1}\|E(y_0)\|^2,$$

which satisfies (2.22) for $k=0$. From the definition of d_k, (2.13), and (2.15), we declare that

$$\begin{aligned}E(y_k)^\top d_k&=-\theta_k^{\mathrm{EOP}}\|E(y_k)\|^2+\beta_k^{\mathrm{EOP}}E(y_k)^\top s_{k-1}\\&=-\left(\zeta_k\left(\Gamma_k^{\mathrm{MSM}}\right)^{-1}+\beta_k^{\mathrm{EOP}}\frac{E(y_k)^\top s_{k-1}}{\|E(y_k)\|^2}\right)\|E(y_k)\|^2+\beta_k^{\mathrm{EOP}}E(y_k)^\top s_{k-1}\\&=-\zeta_k\left(\Gamma_k^{\mathrm{MSM}}\right)^{-1}\|E(y_k)\|^2\leq-\left(\Gamma_{\max}^{\mathrm{MSM}}\right)^{-1}\|E(y_k)\|^2.\end{aligned}$$

The final inequality holds because $\zeta_k=1+\tau_k-\tau_k^2\in[1,5/4]$, since $\tau_k=t_k\in(0,1]$, and $\Gamma_k^{\mathrm{MSM}}\leq\Gamma_{\max}^{\mathrm{MSM}}$. Therefore, (2.22) is satisfied. □

3 Convergence analysis

In this section, we establish the global convergence of the ASPCGP method. Throughout the analysis, we assume that the sequences $\{x_k\}$, $\{y_k\}$, and $\{z_k\}$ are generated by the ASPCGP method, and that the following assumptions hold.

Assumption 3.1.

(i) The solution set Sol_E of unconstrained SoNE (2.1) is nonempty.

(ii) For any $x^* \in Sol_E$ and $x \in \mathbb{R}^n$, it holds that $E(x)^\top (x - x^*) \geq 0$.

Remark 3.1. Assumption 3.1(ii) was originally introduced by Solodov and Svaiter [45] to establish the global convergence of the projection method for the variational inequality problem. Subsequently, this assumption was adopted in [17, 36, 63] to demonstrate the global convergence of projection methods for unconstrained SoNEs. It is worth noting that Assumption 3.1(ii) holds if the mapping E is monotone,

$$[E(x) - E(y)]^\top (x - y) \geq 0, \quad \forall x, y \in \mathbb{R}^n,$$

or pseudo-monotone,

$$E(y)^\top (x - y) \geq 0 \;\Rightarrow\; E(x)^\top (x - y) \geq 0, \quad \forall x, y \in \mathbb{R}^n,$$

but the converse does not necessarily hold. Therefore, Assumption 3.1(ii) is considered less restrictive than requiring the monotonicity or pseudo-monotonicity of the mapping E, as is commonly assumed in most existing DFP methods for solving the SoNE (2.1).

Assumption 3.2. The mapping E is L-Lipschitz continuous.

For convenience, we introduce the following notations:

$$w_k := \|x_k - x^*\|^2, \quad \delta_k := 2\phi_k \|x_k - x_{k-1}\|^2, \tag{3.1}$$

where $x^* \in Sol_E$. In addition, we provide the following identity for use in the subsequent convergence analysis:

$$2(a-b)^\top (c-d) = (\|a-d\|^2 - \|a-c\|^2) + (\|b-c\|^2 - \|b-d\|^2) \tag{3.2}$$

for all $a, b, c, d \in \mathbb{R}^n$.

Lemma 3.1. *Suppose that Assumption* 3.1 *holds and take $x_{-1} = x_0$. Then, for any $x^* \in Sol_E$, it holds that $w_{-1} = w_0$, and*

$$w_{k+1} - w_k \leq \phi_k (w_k - w_{k-1}) + \delta_k - \gamma(2-\gamma)\sigma^2 \frac{\|z_k - y_k\|^4 [\min\{\mu, \nu \|E(z_k)\|\}]^2}{\|E(z_k)\|^2}. \tag{3.3}$$

Proof. From the definition of w_k in (3.1) and the choice $x_{-1} = x_0$, it follows that $w_{-1} = w_0$. Next, we proceed to show that (3.3) holds. By taking Assumption 3.1(ii), $x^* \in Sol_E$,

$z_k = y_k + t_k d_k$, and the adaptive line search (2.16) into account, we have

$$\begin{aligned} E(z_k)^\top (y_k - x^*) &= E(z_k)^\top (y_k - z_k) + E(z_k)^\top (z_k - x^*) \\ &\geq E(z_k)^\top (y_k - z_k) \\ &\geq \sigma t_k^2 \|d_k\|^2 \min\{\mu, \nu \|E(z_k)\|\} \\ &= \sigma \|y_k - z_k\|^2 \min\{\mu, \nu \|E(z_k)\|\} > 0. \end{aligned}$$

Combining this with the definition of x_{k+1} in (2.17) and (2.18), we obtain

$$\begin{aligned} \|x_{k+1} - x^*\|^2 &= \|y_k - \gamma \xi_k E(z_k) - x^*\|^2 \\ &= \|y_k - x^*\|^2 - 2\gamma \xi_k E(z_k)^\top (y_k - x^*) + \gamma^2 \xi_k^2 \|E(z_k)\|^2 \\ &\leq \|y_k - x^*\|^2 - 2\gamma \xi_k E(z_k)^\top (y_k - z_k) + \gamma^2 \xi_k^2 \|E(z_k)\|^2 \\ &= \|y_k - x^*\|^2 - \gamma(2-\gamma) \frac{[E(z_k)^\top (y_k - z_k)]^2}{\|E(z_k)\|^2} \\ &\leq \|y_k - x^*\|^2 - \gamma(2-\gamma) \frac{\sigma^2 \|y_k - z_k\|^4 [\min\{\mu, \nu \|E(z_k)\|\}]^2}{\|E(z_k)\|^2}. \end{aligned} \tag{3.4}$$

It follows from $y_k = x_k + \phi_k (x_k - x_{k-1})$ that

$$\begin{aligned} \|y_k - x^*\|^2 &= \|x_k + \phi_k (x_k - x_{k-1}) - x^*\|^2 \\ &= \|x_k - x^*\|^2 + \phi_k^2 \|x_k - x_{k-1}\|^2 + 2\phi_k (x_k - x^*)^\top (x_k - x_{k-1}) \\ &= \|x_k - x^*\|^2 + \phi_k \big(\|x_k - x^*\|^2 - \|x_{k-1} - x^*\|^2\big) + \big(\phi_k^2 + \phi_k\big) \|x_k - x_{k-1}\|^2 \\ &\leq \|x_k - x^*\|^2 + \phi_k \big(\|x_k - x^*\|^2 - \|x_{k-1} - x^*\|^2\big) + 2\phi_k \|x_k - x_{k-1}\|^2, \end{aligned}$$

where the third equality follows from (3.2), and the last inequality holds due to $0 \leq \phi_k \leq \phi < 1$. By inserting the above inequality into (3.4) and using the definitions of w_k and δ_k in (3.1), it follows that (3.3) holds. This completes the proof. □

Theorem 3.1. *Suppose that Assumption* 3.1 *holds, and let* $x_{-1} = x_0$. *Then, for any* $x^* \in Sol_E$, *the following three results hold:*

(i) The limit $\lim_{k \to +\infty} \|x_k - x^*\|$ *exists.*

(ii) $\sum_{k=0}^{+\infty} \Gamma_k^2 < +\infty$, *where*

$$\Gamma_k = \frac{\|z_k - y_k\|^2 \min\{\mu, \nu \|E(z_k)\|\}}{\|E(z_k)\|}.$$

Furthermore, $\lim_{k \to +\infty} \Gamma_k = 0$.

(iii) The sequences $\{x_k\}$ *and* $\{y_k\}$ *are both bounded.*

Proof. (i) It holds from (3.3) and $\gamma \in (0,2)$ that

$$w_{k+1} - w_k \leq \phi_k (w_k - w_{k-1}) + \delta_k.$$

Let

$$W_k := w_k - w_{k-1}, \quad [\Xi]_+ := \max\{\Xi, 0\}, \tag{3.5}$$

then $W_0 = \delta_0 = 0$ due to $x_{-1} = x_0$. Furthermore,

$$W_{k+1} \le \phi_k W_k + \delta_k \le \phi_k [W_k]_+ + \delta_k.$$

Together with the fact that $0 \le \phi_k \le \phi < 1$, we deduce that

$$[W_{k+1}]_+ \le \phi [W_k]_+ + \delta_k \le \phi^{k+1} [W_0]_+ + \sum_{j=0}^{k} \phi^j \delta_{k-j} = \sum_{j=0}^{k} \phi^j \delta_{k-j}.$$

Then, from $\delta_0 = 0, \phi \in [0,1)$, and (2.21), we have

$$\sum_{k=0}^{+\infty} [W_{k+1}]_+ \le \sum_{k=0}^{+\infty} \left(\sum_{j=0}^{k} \phi^j \delta_{k-j} \right) \le \left(\sum_{j=0}^{+\infty} \phi^j \right) \cdot \left(\sum_{k=0}^{+\infty} \delta_k \right) = \frac{1}{1-\phi} \sum_{k=0}^{+\infty} \delta_k < +\infty. \tag{3.6}$$

Denote $\varpi_k := w_k - \Sigma_{j=1}^{k} [W_j]_+$. From (3.6), it follows that $\{\Sigma_{j=1}^{k} [W_j]_+\}$ is bounded above. Combining this with $w_k \ge 0$, we conclude that $\{\varpi_k\}$ is bounded below. On the other hand, by referencing (3.5), we have

$$\begin{aligned}
\varpi_{k+1} &= w_{k+1} - [W_{k+1}]_+ - \sum_{j=1}^{k} [W_j]_+ \\
&= w_{k+1} - \max\{W_{k+1}, 0\} - \sum_{j=1}^{k} [W_j]_+ \\
&\le w_{k+1} - W_{k+1} - \sum_{j=1}^{k} [W_j]_+ \\
&= w_{k+1} - (w_{k+1} - w_k) - \sum_{j=1}^{k} [W_j]_+ =: \varpi_k.
\end{aligned}$$

This implies that $\{\varpi_k\}$ is non-increasing. So, the limit $\lim_{k\to+\infty} \varpi_k$ exists. Combining this with (3.6), one has

$$\lim_{k\to+\infty} w_k = \lim_{k\to+\infty} \left(\varpi_k + \sum_{j=1}^{k} [W_j]_+ \right) = \lim_{k\to+\infty} \varpi_k + \sum_{j=1}^{+\infty} [W_j]_+ < +\infty,$$

i.e. $\lim_{k\to+\infty} \|x_k - x^*\|$ exists.

(ii) From the definition of Γ_k, (3.3), (3.5), and $0 \le \phi_k \le \phi < 1$, it holds that

$$\begin{aligned}
\gamma(2-\gamma)\sigma^2 \Gamma_k^2 &\le w_k - w_{k+1} + \phi_k (w_k - w_{k-1}) + \delta_k \\
&\le w_k - w_{k+1} + \phi [W_k]_+ + \delta_k.
\end{aligned}$$

By summing the above relation from $k = 0$ to $+\infty$ and utilizing (2.21), (3.1), (3.6), and $\delta_0 = W_0 = 0$, we deduce that

$$\gamma(2-\gamma)\sigma^2\sum_{k=0}^{+\infty}\Gamma_k^2 \le w_0+\phi\sum_{k=0}^{+\infty}[W_k]_+ +\sum_{k=0}^{+\infty}\delta_k$$
$$= w_0+\phi\sum_{k=1}^{+\infty}[W_k]_+ +2\sum_{k=1}^{+\infty}\phi_k\|x_k-x_{k-1}\|^2<+\infty,$$

which completes the proof due to $\gamma\in(0,2)$ and $\sigma>0$.

(iii) Take $x^*\in Sol_E$. By invoking Theorem 3.1(i), we obtain the existence of $\lim_{k\to+\infty}\|x_k-x^*\|$. Consequently, it can be deduced that $\{x_k\}$ is bounded. Moreover, by referring to (2.21), we infer that

$$\lim_{k\to+\infty}\phi_k\|x_k-x_{k-1}\|^2=0,$$

which, along with the inertial step $y_k=x_k+\phi_k(x_k-x_{k-1})$ and $0\le\phi_k\le\phi<1$, suggests that

$$\|y_k-x_k\|^2=\phi_k^2\|x_k-x_{k-1}\|^2\le\phi_k\|x_k-x_{k-1}\|^2\to 0 \quad \text{as} \quad k\to+\infty.$$

Thus, we have

$$\lim_{k\to+\infty}\|y_k-x_k\|=0. \tag{3.7}$$

Hence, we have demonstrated that $\{y_k\}$ is also bounded. □

Lemma 3.2. *Suppose that Assumption* 3.2 *holds. For all $k\ge0$, d_k satisfies the following inequality:*

$$\left(\Gamma_{\max}^{\mathrm{MSM}}\right)^{-1}\|E(y_k)\|\le\|d_k\|\le\left(\frac{5}{4\Gamma_{\min}^{\mathrm{MSM}}}+2\max\left\{\frac{2(L+r)}{r},\varrho\right\}\right)\|E(y_k)\|. \tag{3.8}$$

Proof. From $d_0=-E(y_0)$, we obtain $\|d_0\|=\|E(y_0)\|$, further implies (3.8) holds for $k=0$. Using (2.22) and the Cauchy-Schwarz inequality, we obtain the first inequality in (3.8) holds. Next, we verify that the second inequality in (3.8) is true for $k\ge1$. Consider two cases to prove that the following inequality holds:

$$|\beta_k^{\mathrm{EOP}}|\le\max\left\{\frac{2(L+r)}{r},\varrho\right\}\frac{\|E(y_k)\|}{\|s_{k-1}\|}. \tag{3.9}$$

(A) Given the condition $s_{k-1}^\top p_{k-1}\ge0$, by combining this with the definition of η_{k-1}, we obtain

$$s_{k-1}^\top\eta_{k-1}=s_{k-1}^\top p_{k-1}+r\|s_{k-1}\|^2\ge r\|s_{k-1}\|^2.$$

Applying the L-Lipschitz continuity property of the mapping E, we have

$$s_{k-1}^\top\eta_{k-1}=s_{k-1}^\top p_{k-1}+r\|s_{k-1}\|^2\le(L+r)\|s_{k-1}\|^2,$$

which further implies

$$r\le\Lambda_k^*=\frac{s_{k-1}^\top\eta_{k-1}}{\|s_{k-1}\|^2}\le L+r.$$

According to the definition of β_k^{EOP}, we have

$$\begin{aligned}
\left|\beta_k^{\mathrm{EOP}}\right| &= \left|\frac{E(y_k)^\top(\eta_{k-1}-\Lambda_k^* s_{k-1})}{s_{k-1}^\top \eta_{k-1}}\right| \\
&\leq \frac{\|E(y_k)\|\|\eta_{k-1}\|+\Lambda_k^*\|E(y_k)\|\|s_{k-1}\|}{s_{k-1}^\top \eta_{k-1}} \\
&\leq \frac{\|E(y_k)\|\|\eta_{k-1}\|+(L+r)\|E(y_k)\|\|s_{k-1}\|}{r\|s_{k-1}\|^2} \\
&\leq \frac{\|E(y_k)\|(L+r)\|s_{k-1}\|+(L+r)\|E(y_k)\|\|s_{k-1}\|}{r\|s_{k-1}\|^2} \\
&\leq \frac{2(L+r)\|E(y_k)\|}{r\|s_{k-1}\|}. \qquad (3.10)
\end{aligned}$$

(B) Let $s_{k-1}^\top p_{k-1}<0$. The definition of β_k^{EOP} leads to

$$\beta_k^{\mathrm{EOP}} = \varrho\cdot\frac{\|E(y_k)\|}{\|s_{k-1}\|}. \qquad (3.11)$$

By combining (3.10) and (3.11), we obtain (3.9). It then follows from (2.13)-(2.15), (3.9), and $\zeta_k\in[1,5/4]$ that

$$\begin{aligned}
\|d_k\| &= \left\|-\theta_k^{\mathrm{EOP}}E(y_k)+\beta_k^{\mathrm{EOP}}s_{k-1}\right\| \\
&= \left\|-\left(\zeta_k\left(\Gamma_k^{\mathrm{MSM}}\right)^{-1}+\beta_k^{\mathrm{EOP}}\frac{E(y_k)^\top s_{k-1}}{\|E(y_k)\|^2}\right)E(y_k)+\beta_k^{\mathrm{EOP}}s_{k-1}\right\| \\
&\leq \zeta_k\left(\Gamma_k^{\mathrm{MSM}}\right)^{-1}\|E(y_k)\|+\left|\beta_k^{\mathrm{EOP}}\right|\frac{\|E(y_k)\|\|s_{k-1}\|}{\|E(y_k)\|^2}\|E(y_k)\|+\left|\beta_k^{\mathrm{EOP}}\right|\|s_{k-1}\| \\
&= \zeta_k\left(\Gamma_k^{\mathrm{MSM}}\right)^{-1}\|E(y_k)\|+2\left|\beta_k^{\mathrm{EOP}}\right|\|s_{k-1}\| \\
&\leq \zeta_k\left(\Gamma_k^{\mathrm{MSM}}\right)^{-1}\|E(y_k)\|+2\max\left\{\frac{2(L+r)}{r},\varrho\right\}\frac{\|E(y_k)\|}{\|s_{k-1}\|}\|s_{k-1}\| \\
&= \left(\frac{5}{4\Gamma_{\min}^{\mathrm{MSM}}}+2\max\left\{\frac{2(L+r)}{r},\varrho\right\}\right)\|E(y_k)\|,
\end{aligned}$$

and the proof is completed. □

Theorem 3.2. *Suppose that Assumptions* 3.1 *and* 3.2 *hold. Then* $\{x_k\},\{y_k\}$ *and* $\{z_k\}$ *all converge to a solution of unconstrained SoNE* (2.1).

Proof. We prove this claim by the following three parts.

Part I. We show that $\lim_{k\to+\infty}\|z_k-y_k\|=\lim_{k\to+\infty}t_k\|d_k\|=0$. Recall that, according to Theorem 3.1(iii), $\{y_k\}$ is bounded. Additionally, due to the continuity of the mapping E,

there exists a positive constant N_1 such that

$$\|y_k\| \le N_1, \quad \|E(y_k)\| \le N_1, \quad \forall k \ge 0. \tag{3.12}$$

Combining this with (3.8), we obtain

$$\begin{aligned}\|d_k\| &\le \left(\frac{5}{4\Gamma_{\min}^{\mathrm{MSM}}} + 2\max\left\{\frac{2(L+r)}{r}, \varrho\right\}\right)\|E(y_k)\| \\ &\le \left(\frac{5}{4\Gamma_{\min}^{\mathrm{MSM}}} + 2\max\left\{\frac{2(L+r)}{r}, \varrho\right\}\right)N_1,\end{aligned}$$

which implies that $\{d_k\}$ is bounded. From the definition of z_k and $t_k \in (0,\, \varsigma]$, it follows that $\{z_k\}$ is also bounded. Again, by the continuity of the mapping E, there exists a constant $\hat{N}_1 > 0$ such that

$$\|E(z_k)\| \le \hat{N}_1, \quad \forall k \ge 0.$$

If $\min\{\mu, \nu\|E(z_k)\|\} = \mu$, then

$$\frac{\min\{\mu, \nu\|E(z_k)\|\}}{\|E(z_k)\|} \ge \frac{\mu}{\hat{N}_1}.$$

Otherwise, $\min\{\mu, \nu\|E(z_k)\|\}/\|E(z_k)\| = \nu$. Define

$$\Phi := \min\left\{\frac{\mu}{\hat{N}_1}, \nu\right\} \le \frac{\min\{\mu,\, \nu\|E(z_k)\|\}}{\|E(z_k)\|}.$$

Combining this with Theorem 3.1(ii), we conclude that

$$\|z_k - y_k\|^2 \cdot \Phi \le \frac{\|z_k - y_k\|^2 \min\{\mu, \nu\|E(z_k)\|\}}{\|E(z_k)\|} \;\to\; 0 \quad \text{as} \quad k \;\to\; +\infty.$$

By the definition of z_k, it follows that

$$\lim_{k\to+\infty} \|z_k - y_k\| = \lim_{k\to+\infty} t_k\|d_k\| = 0. \tag{3.13}$$

Part II. We prove that $\liminf_{k\to+\infty}\|E(y_k)\| = 0$. Assume, by contradiction, that $\liminf_{k\to+\infty}\|E(y_k)\| \neq 0$. This implies the existence of a constant $N_2 > 0$ such that

$$\|E(y_k)\| \ge N_2, \quad \forall k \ge 0. \tag{3.14}$$

This, together with (3.8), yields

$$0 < \left(\Gamma_{\max}^{\mathrm{MSM}}\right)^{-1} N_2 \le \|d_k\|, \quad \forall k \ge 0. \tag{3.15}$$

Using (3.15) together with the fact that $\lim_{k\to+\infty} t_k\|d_k\| = 0$, we conclude that $\lim_{k\to+\infty} t_k = 0$. By considering the boundedness of $\{d_k\}$ and $\{y_k\}$, without loss of generality, we assume

$$\lim_{i\to+\infty} y_{k_i} = \overline{y}, \quad \lim_{i\to+\infty} d_{k_i} = \overline{d}. \tag{3.16}$$

Substituting $k:=k_i$ into (2.22), taking the limit of both sides, and using (3.14), (3.16), and the continuity of the mapping E, we have

$$E(\overline{y})^\top \overline{d} \leq -\left(\Gamma_{\max}^{\mathrm{MSM}}\right)^{-1} \|E(\overline{y})\|^2 \leq -\left(\Gamma_{\max}^{\mathrm{MSM}}\right)^{-1} N_2^2 < 0. \tag{3.17}$$

Next, by applying the adaptive line search (2.16) in the ASPCGP method, we have

$$\begin{aligned} -E\left(y_k+\rho^{-1}t_k d_k\right)^\top d_k &< \sigma\rho^{-1}t_k\|d_k\|^2 \cdot \min\left\{\mu,\nu\|E\left(y_k+\rho^{-1}t_k d_k\right)\|\right\} \\ &\leq \sigma\rho^{-1}t_k\|d_k\|^2\cdot\mu. \end{aligned}$$

Taking the limit as $k\to+\infty$ in the above inequality (with $k:=k_i$), and using $\lim_{k\to+\infty} t_k=0$, together with (3.16) and the continuity of the mapping E, we obtain

$$-E(\overline{y})^\top \overline{d} \leq 0,$$

and this contradicts (3.17). Therefore, we conclude that

$$\liminf_{k\to+\infty} \|E(y_k)\| = 0. \tag{3.18}$$

Part III. We prove that $\{x_k\},\{y_k\}$, and $\{z_k\}$ all converge to a solution of the unconstrained SoNE (2.1). Starting from (3.12), (3.18), and using the continuity of the mapping E, we assume, without loss of generality, that

$$\lim_{i\to+\infty} y_{k_i} = \overline{y}, \quad \lim_{i\to+\infty} \|E(y_{k_i})\| = \|E(\bar{y})\| = 0. \tag{3.19}$$

From (3.7), it is easy to see that $x_{k_i}\to\overline{y}$ as $i\to+\infty$. Moreover, the second relation in (3.19) implies that $\overline{y}\in \mathrm{Sol}_E$. By setting $x^* := \overline{y}$ in Theorem 3.1(i), and using the fact that $\lim_{i\to+\infty} x_{k_i} = \overline{y}$, we obtain

$$\lim_{k\to+\infty} \|x_k-\overline{y}\| = \lim_{i\to+\infty} \|x_{k_i}-\overline{y}\| = 0,$$

which implies that the entire sequence $\{x_k\}$ converges to $\overline{y}\in \mathrm{Sol}_E$. Combining this with (3.7) and (3.13), we conclude that both $\{y_k\}$ and $\{z_k\}$ also converge to $\overline{y}$, which completes the proof. □

4 Numerical experiments

In this section, we demonstrate the numerical effectiveness of the ASPCGP method. All code was written in MATLAB R2021b (64-bit) and ran on a Lenovo PC equipped with an Intel(R) Core(TM) i5-1155G7 CPU @ 2.5 GHz, 16 GB of RAM, and the Windows 11 operating system.

4.1 Experiment I: Testing unconstrained SoNEs

In this part, we evaluate the numerical performance of the ASPCGP method on unconstrained SoNEs. The problem dimensions for each problem are 10^4, 5×10^4 and 10^5, respectively.

All test problems were evaluated using seven initial points:

$$x_1=(1,1,\ldots,1)^\top, \quad x_2=\left(\frac{1}{3},\frac{1}{3^2},\ldots,\frac{1}{3^n}\right)^\top, \quad x_3=\left(\frac{1}{2},\frac{1}{2^2},\ldots,\frac{1}{2^n}\right)^\top,$$
$$x_4=\left(0,\frac{1}{n},\ldots,\frac{n-1}{n}\right)^\top, \quad x_5=\left(1,\frac{1}{2},\ldots,\frac{1}{n}\right)^\top, \quad x_6=\left(\frac{1}{n},\frac{2}{n},\ldots,1\right)^\top,$$
$$x_7=\left(1-\frac{1}{n},1-\frac{2}{n},\ldots,0\right)^\top.$$

Let $E(x)=(e_1(x),e_2(x),\ldots,e_n(x))^\top$ be defined, and six problems are described below.

Problem 1. [55] Set $e_i(x)=x_i-\sin(|x_i|-1)$ for $i=1,2,\ldots,n$.

Problem 2. [52] Set $e_i(x)=\exp(x_i)-1$ for $i=1,2,\ldots,n$.

Problem 3. [43] Set

$$e_i(x)=4x_i+(x_{i+1}-2x_i)-\frac{x_{i+1}^2}{3}, \quad i=1,2,\ldots,n-1,$$
$$e_n(x)=4x_n+(x_{n-1}-2x_n)-\frac{x_{n-1}^2}{3}.$$

Problem 4. [52] Set

$$e_1(x)=x_1-\exp\left(\cos\left(\frac{x_1+x_2}{2}\right)\right),$$
$$e_i(x)=x_i-\exp\left(\cos\left(\frac{x_{i-1}+x_i+x_{i+1}}{i}\right)\right), \quad i=2,3,\ldots,n-1,$$
$$e_n(x)=x_n-\exp\left(\cos\left(\frac{x_{n-1}+x_n}{n}\right)\right).$$

Problem 5. [61] Set

$$e_1(x)=2x_1+0.5h^2(x_1+h)^3-x_2,$$
$$e_i(x)=2x_i+0.5h^2(x_i+ih)^3-x_{i-1}+x_{i+1}, \quad i=2,3,\ldots,n-1,$$
$$e_n(x)=2x_n+0.5h^2(x_n+nh)^3-x_{n-1},$$

where $h=1/(n+1)$.

Problem 6. [65] Set $e_i(x)=2x_i-\sin(x_i)$, for $i=1,2,\ldots,n$.

We compare the proposed ASPCGP method with three recent methods, namely IHCGPM [23], MOPCG [42], and IM3TFR1 [18]. For the ASPCGP method, we select the following parameter values: $\mu=0.1,\nu=0.3,\varrho=0.001,r=2,\gamma=1.4,\sigma=1,\varsigma=1,\rho=0.5$, $\phi=0.001,\Gamma_{\min}^{\text{MSM}}=10^{-3},\Gamma_{\max}^{\text{MSM}}=10^{3}$, and $\epsilon_{k+1}=1/(k+1)^2$. For the comparison methods, we adopt the parameter settings as specified in their respective original publications. All methods stop the computation when one of the following two criteria is met: (i) $\|E_k\|\leq 10^{-6}$, and (ii) $\|d_k\|\leq 10^{-7}$, where E_k denotes $E(x_k)$, $E(y_k)$, or $E(z_k)$. The comparison results are listed at `https://www.cnblogs.com/888-8/p/17601054.html`, in which "Init" denotes the initial point, "n" is the dimension of the problem, "Itr" is the number of iterations, "NF" represents the number of function evaluations, "Time" refers to the computation time in seconds, and $\|E^*\|$ is the final norm of $\|E_k\|$ at termination.

To visually illustrate the differences in computation, we utilize performance profiles given by Dolan and Moré [10] to show the "computation time (Time)", "number of function evaluations (NF)" and "number of iterations (Itr)" of the comparison results. The operation mechanism of the performance profile is introduced below, using the "Time" as an example. Let $P=\{p|p \text{ is a test problem}\}$, where each test problem corresponds to a unique combination of the equations $E(x)=0$ and its dimension. Define $S=\{s|s \text{ is an algorithm used to solve test problem}\}$. Denote $T_{p,s}$ as the "Time" required by algorithm $s\in S$ to solve test problem $p\in P$ until termination. The performance ratio is defined as $r_{p,s}=T_{p,s}/\min_{s\in S}T_{p,s}$. If the method fails to successfully solve the test problem, it is considered that $r_{p,s}=2\max\{r_{p,s}|p\in P,s\in S\}$. The performance profile of each method $s\in S$ is defined as

$$\rho_s(\tau)=\frac{1}{n_p}\text{size}\{p\in P:\log_2 r_{p,s}\leq\tau\},$$

where size(A) represents the number of elements in the set A, and n_p denotes the total number of test problems. Generally, a higher curve in the figures indicates better numerical performance. Upon analyzing Figs. 1-3, it becomes apparent that the ASPCGP method shows effective and competitive numerical outcomes. Furthermore, it is worth noting that the IHCGPM method exhibits significant potential in terms of NF.

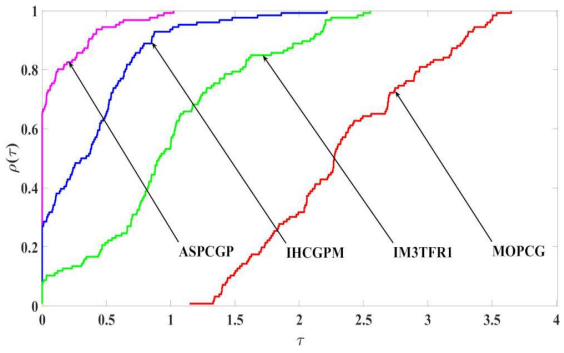

Figure 1: Performance profiles on time.

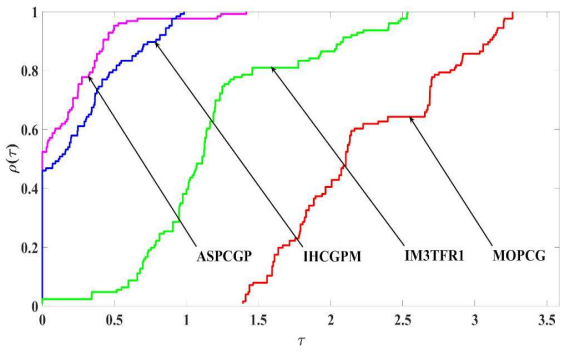

Figure 2: Performance profiles on NF.

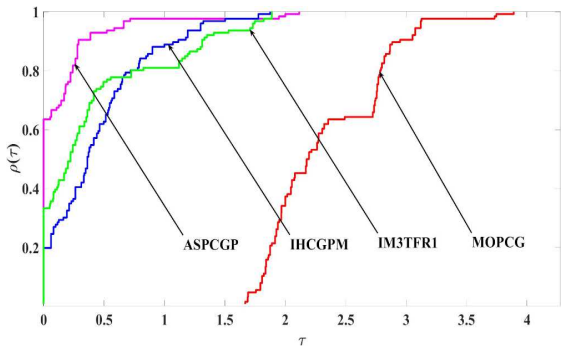

Figure 3: Performance profiles on Itr.

4.2 Experiment II: Application to image de-blurring problems

In this subsection, our objective is to recover the original image from a blurred one using the proposed method. We formulate the problem with the following mathematical model:

$$\min_{x\in\mathbb{R}^n} f(x)=\theta\|x\|_1+\frac{1}{2}\|Ax-b\|^2, \tag{4.1}$$

where $A\in\mathbb{R}^{m\times n}$ is a linear operator, $b\in\mathbb{R}^m$ represents the observed data, and $\theta>0$ is a regularization parameter that balances sparsity and fidelity.

To further address the model (4.1), Figueiredo *et al.* [12] considered a reformulation that transforms it into a bound-constrained quadratic program. This reformulation introduces two auxiliary vectors, $u\in\mathbb{R}^n$ and $v\in\mathbb{R}^n$, which decompose the vector x into two components, i.e., $x=u-v$, where $u_i=\max\{x_i,0\}$ and $v_i=\max\{-x_i,0\}$ for all $i=1,2,\ldots,n$. This decomposition allows us to express $\|x\|_1=\kappa_n^\top u+\kappa_n^\top v$, where $\kappa_n^\top=(1,1,\ldots,1)\in\mathbb{R}^n$. By applying the algebraic theory from [12] and using the first-order optimality condition, we arrive at the following optimization problem:

$$E(Q)=\min\{Q,HQ+C\}=0, \tag{4.2}$$

where

$$Q=\begin{bmatrix}u\\v\end{bmatrix},\quad H=\begin{bmatrix}A^\top A & -A^\top A\\ -A^\top A & A^\top A\end{bmatrix},\quad C=\begin{bmatrix}\theta\kappa_n-A^\top b\\ \theta\kappa_n+A^\top b\end{bmatrix},$$

and H is a semipositive definite matrix. Furthermore, according to [37, Lemma 3] and [54, Lemma 2.2], it is established that the mapping $E:\mathbb{R}^{2n}\to\mathbb{R}^{2n}$ is both Lipschitz continuous and monotone. Expanding upon this framework, we utilize a CG projection-based method to solve problem (4.2), enabling us to effectively address the image de-blurring problem.

During the numerical experiments, we evaluated the performance of our method on a set of tested images, including bridge.bmp (512×512), barbara.png (512×512), fruits.png (512×512), cameraman.png (1024×1024), and hill.png (1024×1024). We refer to [14] for

the background on the digital image restoration problem. In the literature, the quality of restoration is typically measured by the peak signal-to-noise ratio (PSNR)

$$\text{PSNR}=10\times\log_{10}\frac{V^2}{\text{MSE}},\quad \text{MSE}=\frac{1}{MN}\sum_{i=1}^{M}\sum_{j=1}^{N}|x_{i,j}-x^*_{i,j}|^2,$$

where V is the maximum absolute value of the reconstruction, x is the ground truth, x^* is the recovered image, M and N indicate the indicate the image sizes. In addition, we also use the structure similarity index measure (SSIM) [49] as another metric to evaluate image quality, which is given by

$$\text{SSIM}=\frac{(2\mu_u\mu_{\tilde{u}}+C_1)(2\sigma_{u\tilde{u}}+C_2)}{\left(\mu_u^2+\mu_{\tilde{u}}^2+C_1\right)\left(\sigma_u^2+\sigma_{\tilde{u}}^2+C_2\right)},$$

where μ_u and $\mu_{\tilde{u}}$ represent the averages of u and $\tilde{u}$, respectively, σ_u^2 and $\sigma_{\tilde{u}}^2$ are the corresponding variances, $\sigma_{u\tilde{u}}$ represents the corresponding covariance, and C_1 and C_2 are two fixed variables. For a given test image, higher PSNR and SSIM values indicate better performance of the corresponding method. For parameters to ASPCGP method, we select $\mu=0.1,\nu=0.2,\varrho=0.0001,r=0.2,\gamma=1.9,\sigma=0.001,\varsigma=1,\rho=0.6,\phi=0.001,\Gamma_{\min}^{\text{MSM}}=10^{-3}$, $\Gamma_{\max}^{\text{MSM}}=10^3$, and $\epsilon_{k+1}=1/(k+1)^2$. Additionally, to provide a comprehensive comparison, we performed experiments utilizing the MITTCGP [34] and MOPCG [42], while keeping the parameter configurations consistent with their respective original literature. The initialization and stopping criterion of all three methods are exactly the same as the MITTCGP [34]. For a given image x, we generate the data randomly as in [12, 56]. The following MATLAB code illustrates the process:

```
[m, n] = size(x); middle = n / 2 + 1; h = zeros(size(x));
for i = -4 : 4
    for j = -4 : 4
        h(i + middle, j + middle) = 1/(1+i^2 + j^2);
    end
end
h = fftshift(h);
h = h / sum(h(:)); R = @(x) real(ifft2(fft2(h) .* fft2(x)));
b = R(x) + sqrt(6)*randn(size(x)); % Generate noisy blurred observations
```

Table 1 displays the corresponding calculation results of the three methods, while Fig. 4 showcases the blurred images and the restoration results obtained using each of the three methods. For the results presented in Table 1, the **bold text** indicates the best value achieved in solving the corresponding image de-blurring problem. It is evident that the ASPCGP method demonstrates high efficiency and superior restoration quality. Notably, the ASPCGP method outperforms the other two compared methods in terms of PSNR and SSIM for the tested images. These numerical findings demonstrate the application potential of the ASPCGP method in addressing the image de-blurring problem.

Figure 4: The blurred images (first column), the restored images via ASPCGP (second column), MITTCGP (third column) and MOPCG (fourth column), respectively.

Table 1: Numerical results on image restoration.

Image	ASPCGP Itr/Tcpu/PSNR/SSIM	MITTCGP Itr/Tcpu/PSNR/SSIM	MOPCG Itr/Tcpu/PSNR/SSIM
bridge	15/0.92/**25.22**/**0.9121**	52/3.05/24.81/0.8942	**14**/**0.61**/24.71/0.8895
barbara	**12**/**0.56**/**24.75**/**0.8734**	34/1.64/24.29/0.8542	17/0.73/24.52/0.8647
fruits	19/1.11/**31.48**/**0.9379**	34/2.20/30.16/0.9285	**17**/**0.92**/31.29/0.9368
cameraman	**9**/2.86/**39.69**/**0.9943**	16/4.52/37.32/0.9917	10/**2.70**/39.58/0.9942
hill	**12**/**3.88**/**34.55**/**0.9904**	29/8.42/33.49/0.9855	16/4.00/34.30/0.9894

5 Conclusions

In this paper, we present an accelerated spectral Perry-type CG projection (ASPCGP) method for solving unconstrained SoNEs, with applications in image restoration problems. The ASPCGP method defined in this work is an effective extension of the optimal Perry CG-based method. It combines the hyperplane projection method with an acceleration parameter that approximates the Hessian matrix. We prove the global convergence of the proposed method under certain fundamental conditions. Several preliminary numerical experiments and applications demonstrate that the proposed method is practical and promising.

Acknowledgments

The authors would like to sincerely thank the two anonymous referees for their valuable comments, which greatly helped improve the paper.

This work is supported by the National Natural Science Foundation of China (Grant Nos. 72471227, 72071202, and 71971108), by the Jiangsu Province 333 Project (Grant No. (2024)3-0146), by the Natural Science Foundation of Jiangsu Province (Grant No. BK20242012), by the Graduate Innovation Program of China University of Mining and Technology (Grant No. 2025WLKXJ145), and by the Postgraduate Research & Practice Innovation Program of Jiangsu Province (Grant No. KYCX252857).

References

[1] A. B. Abubakar and P. Kumam, *A descent Dai-Liao conjugate gradient method for nonlinear equations*, Numer. Algorithms, 81:197–210, 2019.

[2] A. M. Awwal, P. Kumam, and A. B. Abubakar, *A modified conjugate gradient method for monotone nonlinear equations with convex constraints*, Appl. Numer. Math., 145:507–520, 2019.

[3] A. M. Awwal, P. Kumam, H. Mohammad, W. Watthayu, and A. B. Abubakar, *A Perry-type derivative-free algorithm for solving nonlinear system of equations and minimizing ℓ_1 regularized problem*, Optimization, 70(5-6):1231–1259, 2021.

[4] Z. Chen, W. Cheng, and X. Li, *A global convergent quasi-Newton method for systems of monotone equations*, J. Appl. Math. Comput., 44(1):455–465, 2014.
[5] W. Y. Cheng, *A PRP type method for systems of monotone equations*, Math. Comput. Model., 50(1-2):15–20, 2009.
[6] W. L. Cruz, J. Martinez, and M. Raydan, *Spectral residual method without gradient information for solving large-scale nonlinear systems of equations*, Math. Comput., 75:1429–1448, 2006.
[7] Y. H. Dai and C. X. Kou, *A nonlinear conjugate gradient algorithm with an optimal property and an improved Wolfe line search*, SIAM J. Optim., 23(1):296–320, 2013.
[8] Y. H. Dai and Y. X. Yuan, *A nonlinear conjugate gradient method with a strong global convergence property*, SIAM J. Optim., 10(1):177–182, 1999.
[9] Z. F. Dai, X. H. Chen, and F. H. Wen, *A modified Perry's conjugate gradient method-based derivative-free method for solving large-scale nonlinear monotone equations*, Appl. Math. Comput., 270:378–386, 2015.
[10] E. D. Dolan and J. J. Moré, *Benchmarking optimization software with performance profiles*, Math. Program., 91(2):201–213, 2002.
[11] G. Fasano, F. Lampariello, and M. Sciandrone, *A truncated nonmonotone Gauss-Newton method for large-scale nonlinear least-squares problems*, Comput. Optim. Appl., 34:343–358, 2006.
[12] M. A. T. Figueiredo, R. D. Nowak, and S. J. Wright, *Gradient projection for sparse reconstruction, application to compressed sensing and other inverse problems*, IEEE J. Sel. Topics Signal Process, 1(4):586–597, 2008.
[13] R. Fletcher and C.M. Reeves, *Function minimization by conjugate gradients*, Comput. J., 7(2): 149–154, 1964.
[14] R. C. Gonzales and R. E. Woods, *Digital Image Processing*, Prentice Hall, 2008.
[15] W. J. Hu, J. Z. Wu, and G. L. Yuan, *Some modified Hestenes-Stiefel conjugate gradient algorithms with application in image restoration*, Appl. Numer. Math., 158:360–376, 2020.
[16] A. H. Ibrahim, P. Kumam, A. B. Abubakar, and A. Adamu, *Accelerated derivative-free method for nonlinear monotone equations with an application*, Numer. Linear Algebra Appl., 29(3):e2424, 2022.
[17] A. H. Ibrahim, P. Kumam, B.A. Hassan, A. B. Abubakar, and J. Abubakar, *A derivative-free three-term Hestenes-Stiefel type method for constrained nonlinear equations and image restoration*, Inter. J. Comput. Math., 99(5):1041–1065, 2022.
[18] A. H. Ibrahim, P. Kumam, S. Rapajić, Z. Papp, and A. B. Abubakar, *Approximation methods with inertial term for large-scale nonlinear monotone equations*, Appl. Numer. Math., 181:417–435, 2022.
[19] A. H. Ibrahim, P. Kumam, M. Sun, P. Chaipunya, and A.B. Abubakar, *Projection method with inertial step for nonlinear equations: Application to signal recovery*, J. Ind. Manag. Optim., 19(1):30–55, 2023.
[20] B. Ivanov, G. V. Milovanović, and P. S. Stanimirović, *Accelerated Dai-Liao projection method for solving systems of monotone nonlinear equations with application to image deblurring*, J. Glob. Optim., 85:377–420, 2023.
[21] B. Ivanov, P. S. Stanimirović, G. V. Milovanović, S. Djordjević, and I. Brajević, *Accelerated multiple step-size methods for solving unconstrained optimization problems*, Optim. Methods Softw., 36:998–1029, 2021.
[22] J. B. Jian, L. Han, and X. Z. Jiang, *A hybrid conjugate gradient method with descent property for unconstrained optimization*, Appl. Math. Model., 39:1281–1290, 2015.
[23] J. B. Jian, J. H. Yin, C. M. Tang, and D. L. Han, *A family of inertialderivative-free projection*

methods for constrained nonlinear pseudo-monotone equations with applications, Comput. Appl. Math., 41:309, 2022.

[24] X. Z. Jiang and Z. F. Huang, *An accelerated relaxed-inertial strategy based CGP algorithm with restart technique for constrained nonlinear pseudo-monotone equations to image de-blurring problems*, J. Comput. Appl. Math., 447:115887, 2024.

[25] D. H. Li and M. Fukushima, *A globally and superlinearly convergent Gauss-Newton-based BFGS method for symmetric nonlinear equations*, SIAM J. Numer. Anal., 37(1):152–172, 2000.

[26] J. K. Liu and Y. M. Feng, *A derivative-free iterative method for nonlinear monotone equations with convex constraints*, Numer. Algorithms, 82:245–262, 2019.

[27] J. K. Liu and S. J. Li, *Spectral DY-type projection method for nonlinear monotone system of equations*, J. Comput. Math., 33(4):341–355, 2015.

[28] J. K. Liu, Z. L. Lu, J. L. Xu, S. Wu, and Z. W. Tu, *An efficient projection-based algorithm without Lipschitz continuity for large-scale nonlinear pseudo-monotone equations*, J. Comput. Appl. Math., 403:113822, 2022.

[29] P. J. Liu, L. H. Li, H. Shao, M. X. Liu, and J.X. Fan, *An inertial-type CG projection method with restart for pseudo-monotone costs with application to traffic assignment*, Netw. Spat. Econ., 25(1):147–172, 2025.

[30] P. J. Liu, H. Shao, Y. Wang, and X. Y. Wu, *A three-term CGPM-based algorithm without Lipschitz continuity for constrained nonlinear monotone equations with applications*, Appl. Numer. Math., 175:98–107, 2022.

[31] P. J. Liu, H. Shao, Z. H. Yuan, X. Y. Wu, and T. L. Zheng, *A family of three-term conjugate gradient projection methods with a restart procedure and their relaxed-inertial extensions for the constrained nonlinear pseudo-monotone equations with applications*, Numer. Algorithms, 94:1055–1083, 2023.

[32] P. J. Liu, H. Shao, Z. H. Yuan, and J. H. Zhou, *A family of inertial-based derivative-free projection methods with a correction step for constrained nonlinear equations and their applications*, Numer. Linear Algebra Appl., 31(2):e2533, 2024.

[33] H. K. Lo and A. Chen, *Traffic equilibrium problem with route-specific costs: Formulation and algorithms*, Transp. Res. B: Methodol., 34(6):493–513, 2000.

[34] G. D. Ma, J. C. Jin, J.B. Jian, and D. L. Han, *A modified inertial three-term conjugate gradient projection method for constrained nonlinear equations with applications in compressed sensing*, Numer. Algorithms, 92:1621–1653, 2023.

[35] Y. G. Ou and L. Li, *A unified convergence analysis of the derivative-free projection-based method for constrained nonlinear monotone equations*, Numer. Algorithms, 93:1639–1660, 2023.

[36] Y. G. Ou and W. J. Xu, *A unified derivative-free projection method model for large-scale nonlinear equations with convex constraints*, J. Ind. Manag. Optim., 18(5):3539–3560, 2022.

[37] J. S. Pang, *Inexact Newton methods for the nonlinear complementary problem*, Math. Program., 36(1):54–71, 1986.

[38] A. Perry, *A modified conjugate gradient algorithm*, Oper. Res. Tech. Notes, 26(6):1073–1078, 1978.

[39] B. T. Polyak, *Some methods of speeding up the convergence of iteration methods*, USSR Comput. Math. Math. Phys., 4(5):1–17, 1964.

[40] B. T. Polyak, *The conjugate gradient method in extremal problems*, USSR Comput. Math. Math. Phys., 9:94–112, 1969.

[41] E. Polak and G. Ribière, *Note sur la convergence de méthodes de directions conjuées*, Rev. Fr. Inform. Rech. Oper., 3:35–43, 1969.

[42] J. Sabi'u, A. Shah, P. S. Stanimirović, B. Ivanov, and M. Y. Waziri, *Modified optimal Perry con-*

jugate gradient method for solving system of monotone equations with applications, Appl. Numer. Math., 184:431–445, 2023.

[43] J. Sabi'u, A. Shah, M. Y. Waziri, and M. K. Dauda, *A new hybrid approach for solving large-scale monotone nonlinear equations*, J. Math. Fundam. Sci., 52:17–26, 2020.

[44] M. V. Solodov and B. F. Svaiter, *A globally convergent inexact Newton method for systems of monotone equations*, in: Reformulation: Piecewise Smooth, Semismooth and Smoothing Methods. Applied Optimization, Vol. 22, Springer, 355–369, 1998.

[45] M. V. Solodov and B. F. Svaiter, *A new projection method for variational inequality problems*, SIAM J. Control Optim., 37(3):765–776, 1999.

[46] P. S. Stanimirović and M. B. Miladinović, *Accelerated gradient descent methods with line search*, Numer. Algorithms, 54:503–520, 2010.

[47] M. Sun and J. Liu, *New hybrid conjugate gradient projection method for the convex constrained equations*, Calcolo, 53:399–411, 2018.

[48] X. Y. Wang, S. J. Li, and X. P. Kou, *A self-adaptive three-term conjugate gradient method for monotone nonlinear equations with convex constraints*, Calcolo, 53(2):133–145, 2016.

[49] Z. Wang, A. C. Bovik, H. R. Sheikh, and E. P. Simoncelli, *Image quality assessment: From error visibility to structural similarity*, IEEE Trans. Image Process., 13(4):600–612, 2004.

[50] M. Y. Waziri, K. A. Hungu, and J. Sabi'u, *Descent Perry conjugate gradient methods for systems of monotone nonlinear equations*, Numer. Algorithms, 85:763–785, 2020.

[51] X. Y. Wu, H. Shao, P. J. Liu, Y. Zhang, and Y. Zhuo, *An efficient conjugate gradient-based algorithm for unconstrained optimization and its projection extension to large-scale constrained nonlinear equations with application in signal recovery and image denoising problems*, J. Comput. Appl. Math., 422:114879, 2023.

[52] X. Y. Wu, H. Shao, P. J. Liu, and Y. Zhuo, *An inertial spectral CG projection method based on the memoryless BFGS update*, J. Optim. Theory Appl., 198:1130–1155, 2023.

[53] X. T. Xiao, Y. F. Li, Z. W. Wen, and L. W. Zhang, *A regularized semi-smooth Newton method with projection steps for composite convex programs*, J. Sci. Comput., 76(1):364–389, 2018.

[54] Y. H. Xiao, Q. Y. Wang, and Q. J. Hu, *Non-smooth equations based method for ℓ_1-norm problems with applications to compressed sensing*, Nonlinear Anal. Theory Methods Appl., 74(11):3570–3577, 2011.

[55] Y. H. Xiao and H. Zhu, *A conjugate gradient method to solve convex constrained monotone equations with applications in compressive sensing*, J. Math. Anal. Appl., 405:310–319, 2013.

[56] J. H. Yin, J. B. Jian, and X. Z. Jiang, *A generalized hybrid CGPM-based algorithm for solving large-scale convex constrained equations with applications to image restoration*, J. Comput. Appl. Math., 391:113423, 2021.

[57] J. H. Yin, J. B. Jian, X. Z. Jiang, M. X. Liu, and L. Z. Wang, *A hybrid three-term conjugate gradient projection method for constrained nonlinear monotone equations with applications*, Numer. Algorithms, 88:389–418, 2021.

[58] J. H. Yin, J. B. Jian, and G. D. Ma, *A modified inexact Levenberg-Marquardt method with the descent property for solving nonlinear equations*, Comput. Optim. Appl., 87:289–322, 2024.

[59] G. L. Yuan, T. Li, and W. J. Hu, *A conjugate gradient algorithm for large-scale nonlinear equations and image restoration problems*, Appl. Numer. Math., 147:129–141, 2020.

[60] G. L. Yuan, B. P. Wang, and Z. Sheng, *The Hager-Zhang conjugate gradient algorithm for large-scale nonlinear equations*, Int. J. Comput. Math., 96(8):1533–1547, 2019.

[61] G. L. Yuan and M. J. Zhang, *A three-terms Polak-Ribière-Polyak conjugate gradient algorithm for large-scale nonlinear equations*, J. Comput. Appl. Math., 286:186–195, 2015.

[62] N. Zhang, J. K. Liu, L. Q. Zhang, and Z. L. Lu, *A fast inertial self-adaptive projection based algo-*

rithm for solving large-scale nonlinear monotone equations, J. Comput. Appl. Math., 426:115087, 2023.

[63] L. Zheng, *A new projection algorithm for solving a system of nonlinear equations with convex constraints*, Bull. Korean Math. Soc., 50:823–832, 2013.

[64] G. Zhou and K. C. Toh, *Superlinear convergence of a Newton-type algorithm for monotone equations*, J. Optim. Theory Appl., 125(1):205–221, 2005.

[65] W. J. Zhou and D. H. Li, *Limited memory BFGS method for nonlinear monotone equations*, J. Comput. Math., 25:89–96, 2007.

[66] W. J. Zhou and D. H. Li, *A globally convergent BFGS method for nonlinear monotone equations without any merit functions*, Math. Comp., 77(264):2231–2240, 2008.

[67] W. J. Zhou and D. M. Shen, *Convergence properties of an iterative method for solving symmetric non-linear equations*, J. Optim. Theory Appl., 164(1):277–289, 2015.

[68] W. J. Zhou and F. Wang, *A PRP-based residual method for large-scale monotone nonlinear equations*, Appl. Math. Comput., 261:1–7, 2015.

[69] Z. B. Zhu, Z. Tan, and X. W. Zhu, *An improved inertial projection method for solving convex constrained monotone nonlinear equations with applications*, J. Ind. Manag. Optim., 20 (1):325–346, 2024.